Sensors & Transducers, Vol. 241, Issue 2, February 2020, pp. 1-6

www.sensorsportal.com

Sensors & Transducers

Published by IFSA Publishing, S. L., 2020
http://www.sensorsportal.com

A Multivariate Emissivity Dataset to Facilitate Infrared Thermometry of High Temperature Materials

Eleanor CHALKLEY
Advanced Forming Research Centre, University of Strathclyde, UK
E-mail: eleanor.chalkley@strath.ac.uk

Received: 30 September 2019 /Accepted: 29 January 2020 /Published: 28 February 2020

Abstract: The Advanced Forming Research Centre's Emissivity Calibration Furnace is an instrument designed to provide high volumes of multivariate emissivity data to improve accuracy in infrared radiation thermometry used in metal forming processes. The initial instrument was used create a database of emissivity measurements for commonly used materials. Measurements were carried out on oxidized aluminium, electrical steels, Inconel 718, Ti 6-4, graphite, Waspaloy and various refractory furnace lining materials.

Keywords: Pyrometry, Metals processing, Infrared thermometry, Emissivity.

1. Introduction

In metal forming industries, the key process variable is temperature. This controls the microstructure and material properties of the final product and needs to be measured and controlled throughout. Advances in infrared radiation thermometry mean that it is possible to track the surface temperature of products in metal forming processes from start to finish. However, take up of these technologies is not universal and implementation of infrared temperature measurements can be imperfect, leading to incorrect temperature readings and confusion between contact and non-contact temperature sensing methods.

One cause of poor take up and imperfect implementation is the complexity of accounting for the finite emissivity of metal surfaces. While ratio pyrometry [1] is a mature technology, many sites retain single wavelength or wideband pyrometers, or operate in modes which do not compensate for emissivity, even though specific technologies exist [2]. This leads to internally consistent temperature readings which can be used to repeat a working process, but not to a traceable measurement of temperature which can be used to guide development of processes which require exact temperature control to achieve the target microstructure or material properties. Access to the most applicable emissivity data for each process to improve temperature measurement practices which can improve process efficiency, reduce overall energy usage and increase quality of the final product. Obtaining and broadening access to this data is a priority for manufacturers of non-contact infrared temperature measurement.

1.1. Industrial Infrared Pyrometry

As a centre concentrating on bringing innovative methods to metal forming industries, the AFRC seeks to find ways to improve the application of non-contact infrared thermometry. One approach is to construct a large database of emissivity measurements of various materials of interest to metal processing industries in various conditions, varying in wavelength and temperature.

The equation which forms the basis for ratio pyrometry gives luminance of a body as a function of wavelength and temperature is

$$L(\lambda,T) = \frac{c_1 \varepsilon(\lambda,T)}{\lambda^5\left(e^{\frac{c_2}{\lambda T}}-1\right)}, \qquad (1)$$

where c_1 and c_2 are the combinations of fundamental constants and ε(λ,T) is the emissivity of the surface. The value measured by a pyrometer is the integral of this luminance over the wavelength range that its sensor detects and the solid angle defined by the optics leading to the sensor, referred to as brightness.

A pyrometer is calibrated by measuring the brightness of black body sources (where emissivity is 1.0) at various temperatures. The calibration process gives a formula for converting measured brightnesses to equivalent black body temperatures. The central difficulty of infrared pyrometry can be seen in Eq. 1, which shows that surfaces with lower emissivity will emit radiation that would appear to correspond to a lower temperature than the surface has. Emissivity compensation is now part of most industrial pyrometry systems, but the multivariate and changing nature of the emissivity of hot metal surfaces means that incorrect or inapplicable values are frequently used.

Ratio pyrometers function by measuring $L(T)$ for two wavelengths. If it can be assumed that emissivity of the surface at two wavelengths is equal, then by dividing $L(T)_{\lambda_2}$ by $L(T)_{\lambda_1}$ gives the radiance temperature,

$$T_R = \left(\frac{1}{T} + \frac{\ln(\varepsilon_1/\varepsilon_2)}{c_2(\lambda_2^{-1} - \lambda_1^{-1})}\right). \qquad (2)$$

The assumption that $\varepsilon_1 = \varepsilon_2$ is not always appropriate, especially for surfaces which undergo chemical and physical change during the observed process. The emissivity database identifies these materials and provides the data required to produce high quality pyrometric temperature measurements.

1.2. The Emissivity Calibration Furnace

Eq. 1 also informs the design of an instrument for measuring the emissivity of samples of as-processed metals and high temperature materials. The instrument consists of a regulated tube furnace, a water-cooled freely radiating zone and a freely sliding silicon carbide platform that can accommodate samples of up to 35 × 35 × 10 mm.

The instrument was designed to use dual wavelength ratio pyrometers from the Land Instruments SPOT range to measure the brightness from the sample. The pyrometer remains at a fixed distance from the sample as the sample holder is withdrawn from the effective black body of the tube furnace to the freely radiating water-cooled end zone. The ratio between brightness measured in the hot zone and the water-cooled end zone corresponds to the emissivity of the sample.

The instrument platform and power supply supporting the pyrometers was found to be suitable for accommodating other instruments, and trial measurements using a handheld mid-infrared pyrometer and an 8-14 micron thermal camera were performed. Any instrument with a known bandwidth and an ability to output brightness values (as opposed to temperature values) could therefore be used to construct an emissivity value dataset.

Figure 1 shows the sample positioning for the acquisition of brightness data.

The effective brightness in the hot zone when in thermal equilibrium with the black body furnace includes a reflected contribution from the furnace walls. In opaque solids, ε + R = 1, so the brightness measured with the addition of the reflected black body radiation is the same brightness that would be measured from a sample with ε =1.

The effective brightness in the radiating zone does not include the contribution of reflection from the black body furnace, such that

$$B_{eff} = \varepsilon B = \varepsilon\sigma A(T^4 - T_o^4),$$

where A is a geometric view factor for the sample from the brightness measurement instrument, σ is the Stefan-Boltzmann constant, T is the sample temperature and T_o is the temperature of the cooled radiating zone.

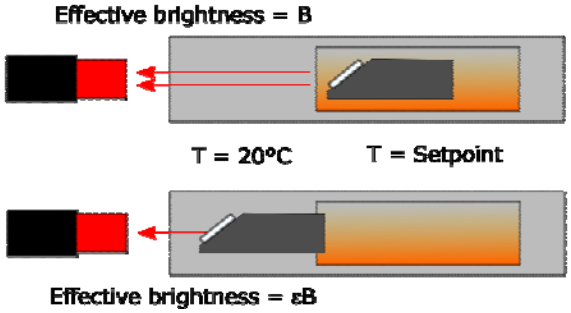

Fig. 1. Schematic of sample positioning during measurement cycle in emissivity calibration furnace usage.

1.3. Materials Surveyed

As well as surveying the range of materials that are processed within the AFRC, a range of refractory and transitional materials were surveyed, including the brick which forms the interior walls of the AFRC's major furnaces, silicon carbide furnace lining and samples of scale developed on materials during heating. The aim of material selection was to improve the practice of thermometry at the AFRC and produce test data for comparison with historical emissivity datasets.

This database aims to extend and improve upon the widely used reference data in Touloukian [3]. Table 1 shows for which materials and temperatures emissivity data was taken. 8-14 µm measurements were performed using a LAND ARC thermal camera, which has a 384 × 288 pixel sensor. Brightness measurements were performed by averaging the

brightness values of the pixels inside the image, which is itself a record of the average emissivity of the surface between 8 µm and 14 µm. To indicate the wide bandwidth nature of the instrument, these measurements are shown as a shaded band on the plot.

The emissivity of refractory brick is used not just in thermometry but in the radiative modelling of furnace heating. Fig. 2 shows the emissivity values measured for a sample of the refractory brick used in the AFRC gas furnace. The manufacturer of the refractory brick quoted a value of 0.85 for the emissivity, which appears to be related to the 8-14 µm value. The change of emissivity with wavelength means that as the furnace temperature increases the heat transfer switches from a radiative to a reflective regime. The current radiative model for the gas furnace does not currently support emissivity values which vary with wavelength, but adding this feature may lead to a closer equivalence between model and furnace.

Table 1. Scope of initial pyrometer-based emissivity data collection.

Material	Wavelengths	Temperature Range
Inconel	1 µm, 1.5 µm, 2.2 µm, 2.4 µm	300 °C to 1100 °C
Titanium	1 µm, 1.5 µm, 2.2 µm, 2.4 µm, 8-14 µm	250 °C to 1100 °C
Aluminium	1 µm, 1.5 µm, 2.2 µm, 2.4 µm, 8-14 µm	250 °C to 550 °C
Waspalloy	1µm, 1.5 µm, 2.2 µm, 2.4 µm, 8-14 µm	300 °C to 1100 °C
Silicon Carbide	1 µm, 1.5 µm	600 °C to 900 °C
Refractory brick	1 µm, 1.5 µm, 2.2 µm, 2.4 µm, 8-14 µm	200 °C to 1050 °C

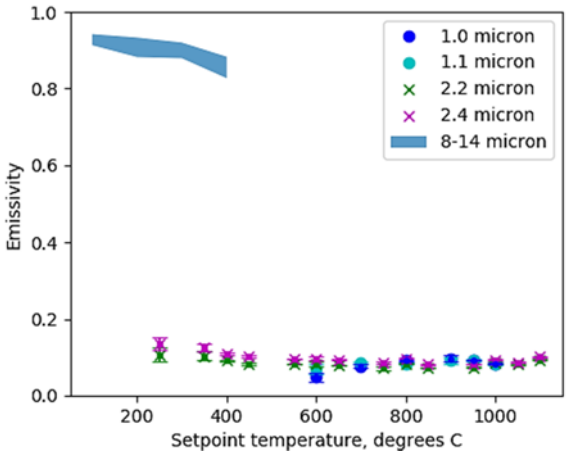

Fig. 2. Emissivity results for alumina refractory brick, as used in the AFRC Gas Furnace, measured at 1.0µm, 1.1 µm, 2.2 µm and 2.4 µm using LAND Spot pyrometers and between 8-14 µm using a LAND ARC thermal camera.

Fig. 3 shows the emissivity measurements of Waspaloy, a nickel-based superalloy with applications in high temperature structures [4]. This material is the closest to a greybody measured during the experimental campaign, with high emissivities at all wavelengths [5]. The material experiences little high temperature change due to heating in air.

Fig. 4 shows the emissivity measurements of a second nickel-based superalloy, the widely used Inconel 718. When heated in air, Inconel 718 develops a dark, matte coating called alpha case [6]. The measurements show that as alpha case grows, the surface emissivity across all wavelengths increases, until around 800 °C, when the surface develops a strong wavelength dependence.

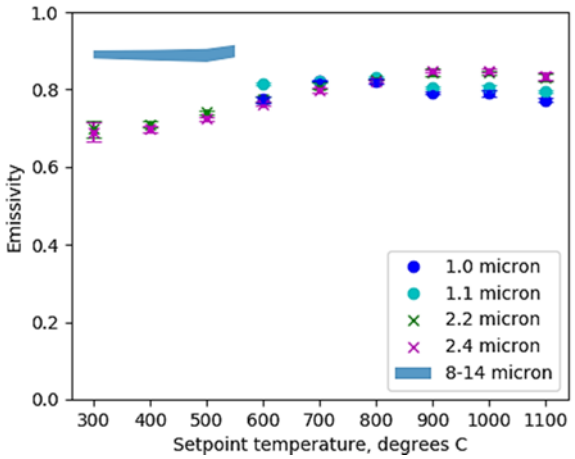

Fig. 3. Emissivity results for Waspalloy in as-received condition, measured at 1.0µm, 1.1 µm, 2.2 µm and 2.4 µm using LAND Spot pyrometers and between 8-14 µm using a LAND ARC thermal camera.

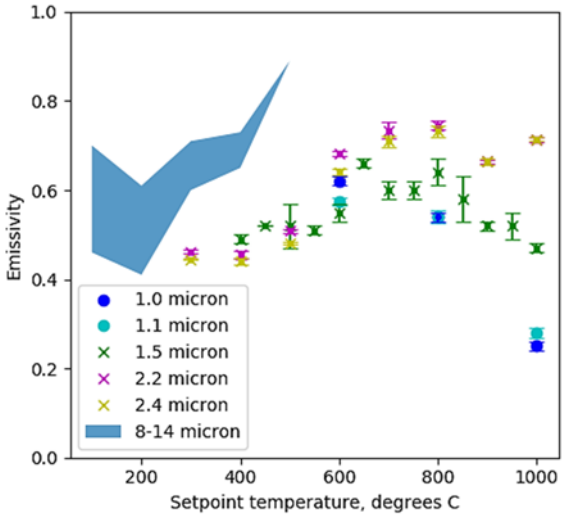

Fig. 4. Emissivity results for Inconel 718 in as-received condition, measured at 1.0µm, 1.1 µm, 1.5 µm, 2.2 µm and 2.4 µm using LAND Spot pyrometers and between 8-14 µm using a LAND ARC thermal camera.

Titanium is forged with and without glass lubricant coatings to control die filling and thermal behaviour [7]. Fig. 5 shows emissivity measurements for titanium sheet coated in Prince Minerals 872207 and titanium sheet in as-received condition at 1.5 µm and 8-14 µm. The emissivity of the coated titanium has a much higer variability during the heating cycle until it passes the glass transform point above 600 °C. The coating also had a higher long wavelength emissivity at low temperatures, but due to the measurement range of the 8-14 µm camera data was not available above the glass transformation temperature.

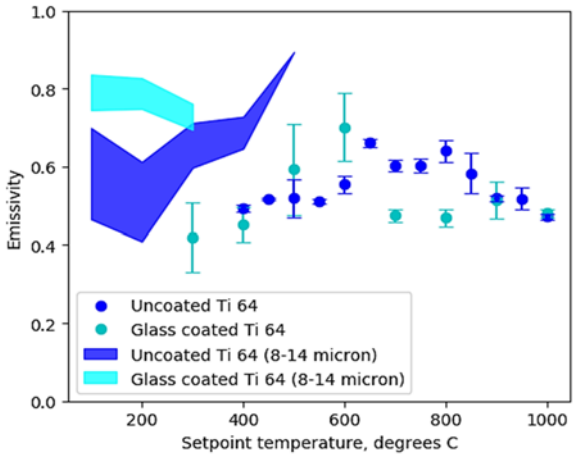

Fig. 5. Comparison of emissivity measured for titanium surfaces with and without glass forging coatings at 1.5 µm using a LAND Spot pyrometers and between 8-14 µm using a LAND ARC thermal camera.

Measurements of oxidised surfaces of various aluminium alloys formed a large part of the experimental campaign.

Fig. 6 shows emissivity values measured for aluminium 1050 which had been heated in air and were considered to be fully oxidised. Measurements at 1.0 µm were not possible below the pyrometer's minimum temperature of 550 °C. A summary of the 2.2 µm emissivity measurements for other aluminium alloys – 2023, 5251, 6082 and 7075 is shown in Fig. 7. The aim of the measurements of aluminium alloys was to establish if the relationship between emissivity, wavelength and temperature was significantly different for different aluminium alloys.

Microalloyed steels were the final material of interest, with measurements carried out on C42 MOD samples, shown in Fig. 8. The samples experienced significant oxidization during heating cycles, motivating the development of a vacuum heating system for future upgrades to the emissivity calibration furnace.

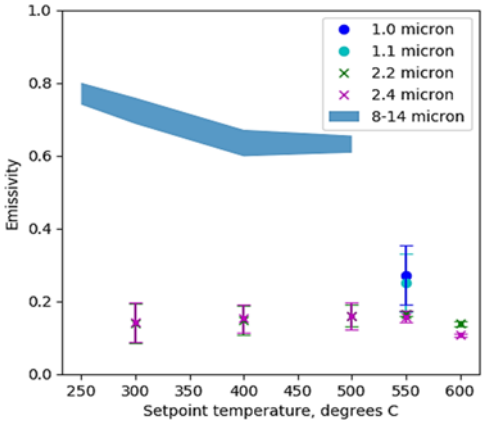

Fig. 6. Emissivity results for aluminium 1050 in as-received condition, measured at 1.0µm, 1.1 µm, 1.5 µm, 2.2 µm and 2.4 µm using LAND Spot pyrometers and between 8-14 µm using a LAND ARC thermal camera.

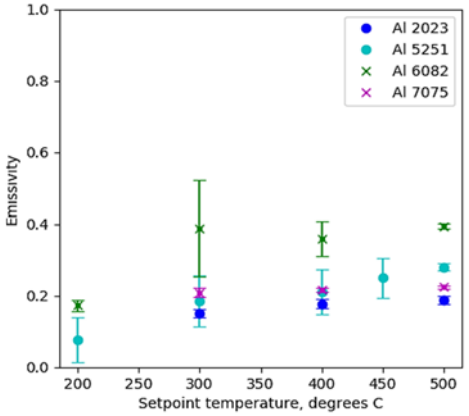

Fig. 7. Emissivity results for various alumiumium alloys in as-received condition, measured at 2.2 µm using LAND Spot pyrometers.

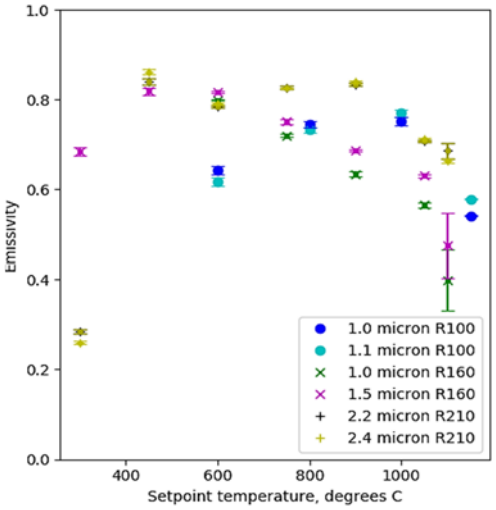

Fig. 8. Emissivity results for C42 MOD steel heated in air, measured at 1.0µm, 1.1 µm, 1.5 µm, 2.2 µm and 2.4 µm using LAND Spot pyrometers.

2. Spectroscopic Emissivity Measurement

With only measurements at the wavelengths that correspond to the specific optics setup of the pyrometers, the emissivity dataset is limited in scope and also in speed of acquisition. Acquiring continuous spectra in addition to the pyrometry wavelengths allows greater data-gathering speed and examination of wavelength-dependent features.

Existing pyrometer optics were adapted to accommodate a ZrF optical fibre which feeds a spectrometer with measurement range from 900 nm to 2500 nm. The short wavelength accuracy limit of the spectrometer measurement is related to the cut-on wavelength of the black body curve.

A custom measurement program was written to produce spectra at 100 ms intervals while the sample was moved out of the black body zone and into the freely radiating cooled zone. This provides a brightness value for every frequency bin, allowing the emissivity to be calculated from the brightness ratio as with a single wavelength pyrometer calculation.

The comparison plot in Fig. 9 shows the emissivity measurements for the wavelengths measured by the three ratio pyrometers plotted alongside the spectrometer data for the same material at the same temperature and an indication of the emissivity range from a reference source [3]. The spectrometer method of emissivity measurement recorded consistently lower values than the band limited and historical data on the Inconel test material.

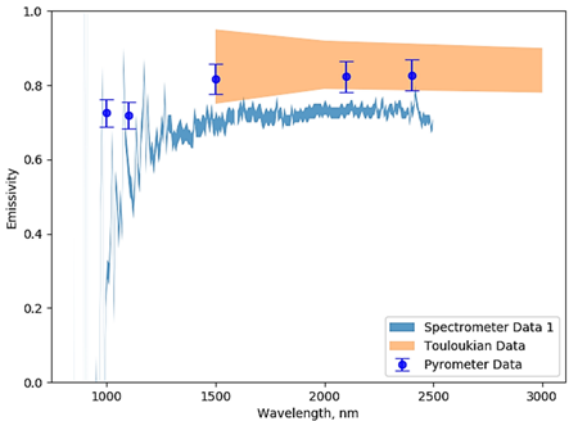

Fig. 9. Comparison of pyrometer and spectrometer measurements of the emissivity of heavily oxidised Inconel 718 at 900 °C with reference data from [3].

This discrepancy caused uncertainty over the efficacy of the spectroscopic measurement method. Further tests were carried out on two materials which were not expected to experience changes in emissivity with temperature – refractory furnace lining brick and oxidized graphite. The emissivity measurements shown in Fig. 10 and Fig. 11 were also carried out in a single heating cycle, by switching the instruments at each temperature setpoint.

The experimental procedure used to obtain the data in Fig. 9 involved measuring samples sequentially as furnace temperature increased, with different instruments used in different heating cycles. Despite the samples being cut from the same sheet, variations in the heating time for each measurement cycle resulted in oxide layers forming differently for each measurement, leading to different emissivity measurements.

The relationship between emissivity and the exact thickness of oxide layers is a topic for future research.

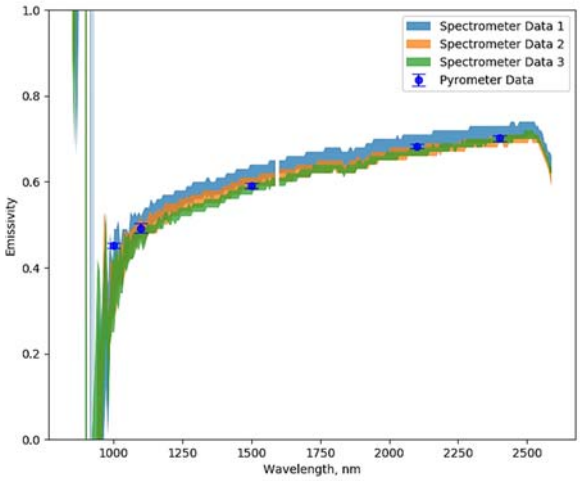

Fig. 10. Comparison of pyrometer and spectrometer measurements of the emissivity of heavily oxidised graphite.

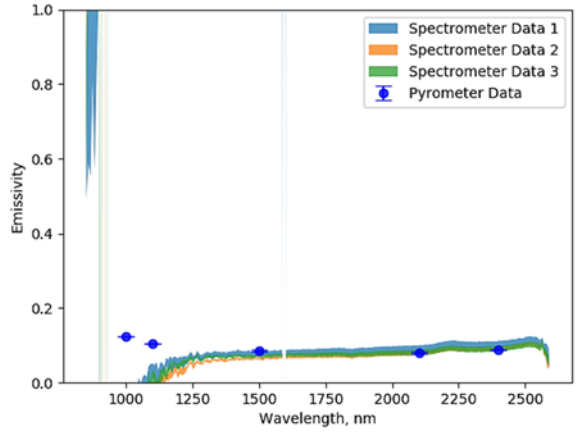

Fig. 11. Comparison of pyrometer and spectrometer measurements of the emissivity of alumina-based refractory ceramic tile.

3. Sample Surface Changes

The furnace is equipped with a gas flow system in order to produce altered atmospheres by continuous flow of gas over the sample.

However, the method of construction of the emissivity calibration furnaces means that the experimental chamber is not gas tight. The silicon carbide sample holder is moved by rods, which also maintain the fixed distance to the pyrometer. These

rods run through holes in the front flange of the tube furnace as shown in Figure 12.

Electrical steels were materials of interest during the measurement campaign and exhibited surface change by oxidization during heating. This was observed during the measurement campaign as an increasing emissivity value above 700 °C.

Fig. 13 shows that the measurements carried out under N2 flow diverge from the measurements carried out in air from 700 °C. Visual inspection of the samples after the trials indicated that the reduced oxygen atmosphere caused by the N2 flow had reduced some of the growth of oxide during heating, but that these conditions were not adequate to produce oxygen-free measurements of surfaces.

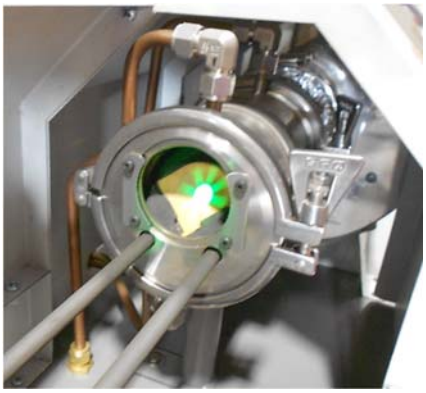

Fig. 12. The front flange of the Emissivity Calibration furnace, showing optical port and sample movement rod holes.

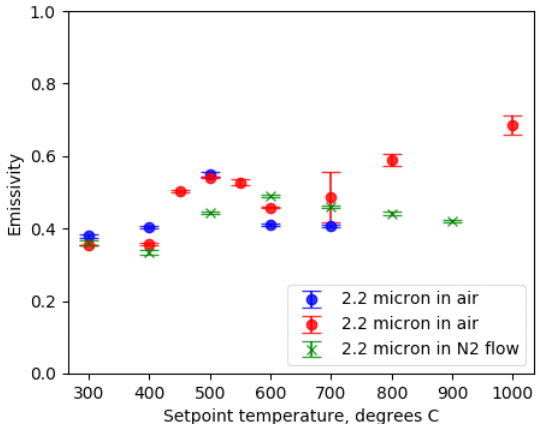

Fig. 13. Emissivity data for electrical steel samples measured at 2.2 microns in air and positive pressure N2 atmospheres.

4. Conclusions

The emissivity calibration furnace was developed and materials including Inconel 718, waspaloy, C42 MOD microalloyed steel, titanium and refractory brick were measured at a range of temperatures across standard wavelengths for infrared non-contact temperature measurements.

Measurements were carried out in a standard air atmosphere, where materials which oxidise were observed to change emissivity during this process. Tests of the gas flow system were made, providing avenues for further improvement of the instrument.

This article was based on a talk given by the author at SEIA 2019 [8].

Acknowledgements

Instruments for the measurement of emissivity and some experimental samples were provided by Land Instruments. The experimental campaign was funded by contributions from Catapult and Land Instruments.

References

[1]. Gibson, A F., A two-colour infra-red radiation pyrometer, *Journal of Scientific Instruments,* Vol. 28, No. 5, 1951, p. 28-153.

[2]. F. Turner, Smart aluminium temperature sensors for Industry 4.0, *Aluminium International Today*, 2018, Vol. 31, Issue 3, pp. 25-27.

[3]. Touloukian, Y. S., DeWitt, D. P., Thermophysical Properties of Matter - The TPRC Data Series. Vol. 7. Thermal Radiative Properties - Metallic Elements and Alloys, *IFI/PLENUM*, New York-Washington, 1970. https://apps.dtic.mil/dtic/tr/fulltext/u2/a951941.pdf

[4]. S. Mannan, S. Patel and J deBarbadillo, Long Term Thermal Stability of Inconel Alloys 718, 706, 909 and Waspaloy at 593°C and 704°C, in Superalloys 2000, *The Minerals, Metals and Materials Society,* Champion, Pennsylvania, 2000, pp. 449-458.

[5]. You-Wen Zhang, Cai-Gen Zhang, and Victor Klemas, Quantitative measurements of ambient radiation, emissivity, and truth temperature of a greybody: methods and experimental results, *Applied Optics,* 20, 1986, pp. 3683-3689.

[6]. Dini, J. W., Chemical Milling, *International Metallurgical Review*, Vol. 20, 1, 1975, pp. 29-56.

[7]. Shivpuri, Rajiv and Kini, Satish, Lubricants and Their Applications in Forging, in Metalworking: Bulk Forming, S.L. Semiatin (Ed.), *ASM Handbook*, 2005, Vol. 14A, pp. 84-92.

[8]. Chalkley, E., A Multivariate Emissivity Database for Industrial Infrared Radiation Thermometry, in *Proceedings of the 5th International Conference on Sensors and Electronic Instrumentation Advances,* 25-27 September 2019, Tenerife, Spain. 2019, pp. 123-125.

[9]. Baker, T. N. Microalloyed steels, 2015, Vol. 43, 4, *Ironmaking & Steelmaking. Processes, Products and Applications*, Vol. 43, Issue 4, 2016, pp. 264-307.